





## Article

# Air Quality Improvement Following the COVID-19 Pandemic Lockdown in Naples, Italy: A Comparative Analysis (2018–2022)

Alessia Sannino <sup>1,†</sup>, Riccardo Damiano <sup>1,†</sup>, Salvatore Amoruso <sup>1,2</sup>, Pasquale Castellano <sup>3</sup>,  
Mariagrazia D'Emilio <sup>4</sup> and Antonella Boselli <sup>4,\*</sup>

<sup>1</sup> Dipartimento di Fisica “Ettore Pancini”, Università di Napoli Federico II, Complesso Universitario di Monte S. Angelo, I-80126 Napoli, Italy; alessia.sannino@unina.it (A.S.); riccardo.damiano@unina.it (R.D.); salvatore.amoruso@unina.it (S.A.)

<sup>2</sup> Institute for SuPerconductors, INnovative Materials, and Devices, Consiglio Nazionale delle Ricerche, UOS Napoli, Complesso Universitario di Monte S. Angelo, I-80126 Napoli, Italy

<sup>3</sup> ALA Advanced Lidar Applications s.r.l., Corso Meridionale 39, I-80143 Napoli, Italy; p.castellano@alasytems.it

<sup>4</sup> Istituto di Metodologie per l'Analisi Ambientale, Consiglio Nazionale delle Ricerche, I-85050 Potenza, Italy; mariagrazia.demilio@cnr.it

\* Correspondence: antonella.boselli@cnr.it

† These authors contributed equally to this work.

**Abstract:** The pandemic lockdown of the year 2020 has been generally accompanied by an improvement in the air quality. Here, we report data on the effects of lockdown limitations on the air quality in the metropolitan area of Naples (Italy) by following the evolution of main atmospheric pollutants over a five-year period and comparing their concentrations in the pandemic year 2020 with the previous (2018 and 2019) and following (2021 and 2022) two years. In particular, NO<sub>2</sub> and PM10 concentrations registered by representative air quality sampling station network and the columnar features of the aerosol characterized by a sun-photometer are considered. To avoid the possible influence of Saharan dust transport, which generally affects the observational area, the analysis has been limited to the days free from such events. Our findings evidence a tendency towards pre-pandemic conditions, notwithstanding some differences related to partial and temporary restrictions imposed even in the year 2021. For both near-surface NO<sub>2</sub> and PM, the observations confirm a significant reduction induced by the lockdown in 2020, besides the seasonal changes, and a gradual tendency towards more typical values in the following years. Also, the columnar aerosol data clearly highlight a gradual recovery of typical conditions in 2021 and 2022, confirming a peculiar effect of the pandemic lockdown of the year 2020 on the atmospheric aerosol characteristics that evidences a striking predominance of the fine component.

**Keywords:** human impact; air quality; remote sensing; post-lockdown effects; COVID-19



**Citation:** Sannino, A.; Damiano, R.; Amoruso, S.; Castellano, P.; D'Emilio, M.; Boselli, A. Air Quality Improvement Following the COVID-19 Pandemic Lockdown in Naples, Italy: A Comparative Analysis (2018–2022). *Environments* **2024**, *11*, 167. <https://doi.org/10.3390/environments11080167>

Academic Editors: Sripriya Nannu Shankar, Tara Sabo-Attwood, Jana S. Kesavan and Sanghee Han

Received: 19 June 2024

Revised: 24 July 2024

Accepted: 3 August 2024

Published: 6 August 2024



**Copyright:** © 2024 by the authors. Licensee MDPI, Basel, Switzerland. This article is an open access article distributed under the terms and conditions of the Creative Commons Attribution (CC BY) license (<https://creativecommons.org/licenses/by/4.0/>).

## 1. Introduction

Human activities display direct impacts on the environment, influencing the balance of ecosystems. The effects of such alterations on the self-adaptive cycle of the ecosystem have become increasingly heavy, generating irreversible imbalances and increasing side effects on the survival of living species [1–5]. Among these human activities, one can quote, for example, intensive livestock farming, deforestation, and uncontrolled emissions of greenhouse gases [6–10], which today are unanimously indicated as causes of “climate change”. Interventions for the mitigation of these changes are still uncertain nowadays and are expected in future decades, whereas the evidence of catastrophic effects increases [11,12]. During the initial phase of the SARS-CoV-2 pandemic, lockdown measures were settled in many countries to cope with the spread of the virus, offering a unique opportunity to somehow clarify the anthropogenic impact on the ecosystem, since in that period, the usual

human activities were strongly limited. In Italy, as in other parts of the world, free access to vaccines and compliance with anti-contagion regulations by a large part of the population progressively led to a situation of gradual and almost total restoration of working and social activities at the end of the year 2020, although the pandemic was not yet over at the end of 2021.

Besides the desired effect of reducing the virus circulation, the lockdown period produced the opportunity to obtain clearer evidence of direct connections between humans and the environment as a secondary effect, although it only lasted for about 2 months in Italy. In fact, numerous environmental studies were carried out in different parts of the world, highlighting water and air quality improvements by comparing observations made during the lockdown with data referring to the same period in the previous year [13–21]. Changes in the air quality during the period of lockdown were quantified, studying possible effects of traffic emissions in Almaty (Kazakhstan), one of the most polluted large cities in the world [22], as well as in China, the first country struck by the SARS-CoV-2 pandemic [23,24]. The lockdown effects on the atmosphere were observed even in the remote region of the Himalayas, a focal point zone for addressing climate changes [25].

In a previous report, soon after the lockdown phase, we investigated its effects on the air quality and the composition of the atmospheric aerosol in the metropolitan city of Naples [26]. By comparing air quality data registered during the lockdown with those of the previous years, we gained evidence of a significant reduction in NO<sub>2</sub>, CO, and SO<sub>2</sub> in predominantly urban or industrial areas of the city, correlated with the reduction in secondary processes and the emission sources of these pollutants. We observed a simultaneous, drastic increase in the fine component in the volume size distribution of the aerosol in the atmospheric air column. Strikingly, few studies seem to have examined the variation in the air quality in the post-lockdown phase in the Mediterranean area [27,28]. This motivated us to analyze the occurrence of changes in local air quality during the recovery phase of human activities by comparing atmospheric parameters over the five-year period from 2018 to 2022 with the pandemic year sitting in the middle.

In continuity with our previous study, which considered the changes that occurred in the pandemic year 2020 with respect to the previous year, we considered both near-surface and remote sensing data over a longer period. In particular, ground level concentrations of PM<sub>10</sub> and NO<sub>2</sub>, provided by monitoring stations of the agency for the environment of the Campania Region [29] located in the city of Naples, were used for the near-surface characterization, whereas the microphysical properties of the atmospheric particulate integrated over the column were characterized by resorting to the AERONET (Aerosol Robotic NETwork) sun-sky-lunar photometer located at the University of Naples Federico II.

## 2. Materials and Methods

Data collected from in situ and remote sensing instruments were separated into two temporal subsets, defined in analogy with the lockdown and pre-lockdown periods that occurred in 2020 and were considered in our previous work [26]. In this respect, it is worth recalling that the pandemic lockdown in the Campania Region lasted from 13 March 13 to 4 May 2020.

Due to its location, the city of Naples is affected by frequent dust transport events from the nearby Saharan regions that can strongly influence experimental findings. Therefore, in order to carry out an analysis free from such atmospheric aerosol components, we identified the days affected by dust events by using the daily dust forecast model provided by the Barcelona Supercomputing Center (<https://dust.aemet.es/> accessed on 14 June 2024) and subsequently verifying the relative aerosol sources through air mass back-trajectories calculated by the HYSPLIT dispersion model (<https://www.ready.noaa.gov/> accessed on 14 June 2024) provided by NOAA Air Resources Laboratory (ARL). Hence, days recognized as being affected by Saharan dust events were removed from the datasets used in the analysis.

Besides Saharan dust events, meteorological conditions might also have an influence on the experimental findings. In fact, changes in weather conditions can lead to a mod-

ification of pollutant emissions, thus affecting air quality. In order to take into account the possible influence of meteorological conditions on the measured data, we partially followed the procedure described by Shi et al. in [30]. In the following analysis, the first period, indicated as “Pre-Lockdown”, refers to the time interval from 1 January to 12 March of each year. For the second period, corresponding to the time interval for which lockdown occurred in the year 2020, the first week was skipped and pollutant data collected in the time range spanning from 20 March to 30 April, dubbed as “Lockdown”, were considered. The corresponding data values were labelled as P-(year) and L-(year), where “(year)” denotes the year to which they refer to. The two P and L temporal datasets were formed both for the pandemic year 2020 and for the previous and following two years (i.e., 2018, 2019, 2021, and 2022), in which there were no strict confinement regulations at the national level, for the sake of comparison of the air quality parameters over the five-year period.

### 2.1. Near-Surface Data

As in our previous work, we considered data at ground level provided by several representative sampling stations of the Agenzia Regionale per la Protezione Ambientale in Campania (ARPAC) monitoring network. Here, we focused and restricted our analysis to PM<sub>10</sub> and NO<sub>2</sub> values registered in three representative locations of the city. This choice was primarily motivated by the key role of NO<sub>2</sub>, which has been identified not only as a principal indicator of pollution resulting from human activities but also as being among the most harmful to health, due to the strong correlation between high levels of NO<sub>2</sub> and increase in mortality risk [31,32]. Moreover, PM is also an important indicator of air quality, with both important environmental and health impacts. The three sampling stations selected are representative of different parts of the city. The first one is located in the suburban green area annexed to the Astronomical Observatory (AO), sitting in the hilly area of Capodimonte, and it is mainly representative of a natural area affected by contamination of anthropogenic activities, even to a minimal extent. The other two stations are instead situated in two areas characterized by a predominance of processes and aerosols related to urban activities and traffic or associated with activities connected to the presence of industries, respectively. In particular, the station located at the National Museum (NM) is in the city center, while the one at Argine Street (AS) is close to the industrial district of the eastern suburbs of Naples.

Even if PM<sub>10</sub> is more linked to the coarse anthropogenic and coarse natural aerosols (desert dust, volcanic plume), while PM<sub>2.5</sub> is more affected by anthropogenic primary emissions and secondary processes triggered by combustion, both PM indicators can be affected by concentrations of particles originating from vehicles. Here, we chose to focus on the PM<sub>10</sub> variation after removing the main natural aerosol source; in fact, due to the different background of the investigated city areas, the change in PM<sub>2.5</sub> was not visible in all sampled sites but only in the busiest area (MN), in agreement with the experimental findings of Speranza and Caggiano [33].

Following our previous analysis, the NO<sub>2</sub> and PM<sub>10</sub> content at ground level for the period from January to April 2020 was compared with the values observed during the same temporal interval of the years 2018, 2019, 2021, and 2022. In each year and for the P and L datasets, we separately analyzed the variation over the five-year period of the daily average of the two pollutant concentrations  $x_P$  and  $x_L$ , measured by the three ARPAC stations. Then, the behavior of the relative variation  $\Delta x_r = (x_L - x_P)/x_P$  between the two periods was analyzed. This last choice was made to avoid any bias in the analysis due to transition phases in the atmosphere.

### 2.2. Remote Sensing Data

Information on the atmospheric column was obtained by resorting to aerosol data provided by the sun-sky-lunar photometer (CIMEL E318T), which has operated in the frame of the global AERONET network decree [34] since 2016 and is located at the Center for Metrological and Technological Services (CeSMA) of the University of Naples Federico

II. AERONET is a federation of more than 400 ground-based sun-sky-lunar photometers placed in more than 50 countries over the world, measuring aerosol radiative, optical, and microphysical properties for continuous atmospheric characterization on local and global scales. The sun-sky-lunar photometer is particularly relevant since the data registered at ground level may not be completely illustrative of the atmospheric situation [35]. Moreover, the parameters retrieved from the sun-sky-lunar photometer remote sensing observations also provide interesting information on the optical and microphysical properties of the aerosol. This instrument collects data at 8 different wavelengths in the spectral range from 340 to 1640 nm and allows us to characterize the columnar aerosol properties through inversion procedures [36], providing columnar aerosol optical depth (AOD) and many other AOD-related products.

For such an analysis, we considered the values of the AOD at 440 nm for quantitative information on the aerosol abundance; in fact, this parameter is reliable and useful to remotely investigate aerosol load and distribution in the atmosphere [37,38]. In particular, the AOD is proportional to the absorbing and scattering particle total loading over the whole atmospheric column and depends on the aerosol mass concentration, size distribution, shape, and complex refractive index. Its wavelength dependence varies with aerosol source and characteristics and can be used to distinguish different aerosol types; it is known that fine-mode particles cause larger variations in the AODs at shorter wavelengths than those caused by coarse-mode particles [38]. The AOD spectral variability is characterized by the Ångström exponent  $\alpha$ , defined as  $\alpha = -\log(\text{AOD}_{\lambda_1}/\text{AOD}_{\lambda_2})/\log(\lambda_1/\lambda_2)$ ,  $\lambda_1$  and  $\lambda_2$  being two different wavelengths [39]. This parameter depends on the aerosol size and increases as the particle size decreases. The columnar  $\alpha$  values, estimated from the AOD ratio at 440 nm/870 nm, can be reliably used for a characterization of the aerosol typology [40] and are typically exploited because they provide information on the coarse versus fine mode aerosol relative influence [41]. Moreover, the particle size distributions per volume, defined as  $(dV(r))/(d\ln(r)) = V(r) dN(r)/d\ln(r)$  (in  $\mu\text{m}^3\mu\text{m}^{-2}$ , where  $r$  is the particle radius and  $dN(r)/d\ln(r)$  is the particles number distribution), was also analyzed to highlight any change that occurred in the aerosol fine and coarse mode fractions [42]. These aerosol parameters were obtained by the level 1.5 (cloud-screened) AERONET data (<https://aeronet.gsfc.nasa.gov/> accessed on 19 April 2024) [43,44]. As already stated above, Saharan dust events were removed from the dataset, and the data from January to April of each year were collected in two subsets corresponding to the P and L time intervals. The final statistical datasets comprised 32 and 12 daily mean values for the P and L intervals in 2018, 46 and 31 for 2019, 22 and 7 for 2020, 31 and 29 for 2021, and 50 and 17 for 2022, respectively.

### 3. Results

Hereafter, we illustrate the results of our analysis on the air quality in the period from January to April for the years 2018, 2019, 2021, and 2022, comparing the data with the corresponding values registered in the same period of the year 2020, affected by the pandemic spread and lockdown. We will first discuss the data obtained from the daily averaged values of the major pollutants  $\text{NO}_2$  and  $\text{PM}_{10}$  registered at ground level by the three selected ARPAC monitoring stations. Then, we will discuss the results for the air column obtained by the sun-sky-lunar photometer. In both cases, we will carry out a comparison highlighting the changes occurring in the parameters of the air quality over the five-year period.

We first discuss the observation related to  $\text{NO}_2$ . Figure 1 reports the data of the  $\text{NO}_2$  concentration registered by the three ARPAC stations in the pre-lockdown (a) and lockdown (b) periods defined above in terms of statistical box plots, as well as their relative variations (c) for the five years under study. The number of days for each year on which  $\text{NO}_2$  measurements were available were between 40 and 70 for each station for pre-lockdown periods, while up to 30 days of measurement were available during lockdown periods. Figure 1a shows that in the pre-lockdown period,  $\text{NO}_2$  did not exhibit noticeable change

over the five years besides the lower values registered at the Astronomico Observatory (AO), which was located in an area less affected by anthropogenic activities with respect to the other two stations. Instead, the data of the lockdown period in Figure 1b evidence a clear reduction in NO<sub>2</sub> in the pandemic year 2020. In particular, one can observe an almost twofold reduction in NO<sub>2</sub> for all three stations, and the two sampling stations located in the areas of the city more influenced by urban and industrial activities display values close to what is normally registered by the Astronomico station, which is representative of a more natural area characterized by a lower anthropogenic influence.

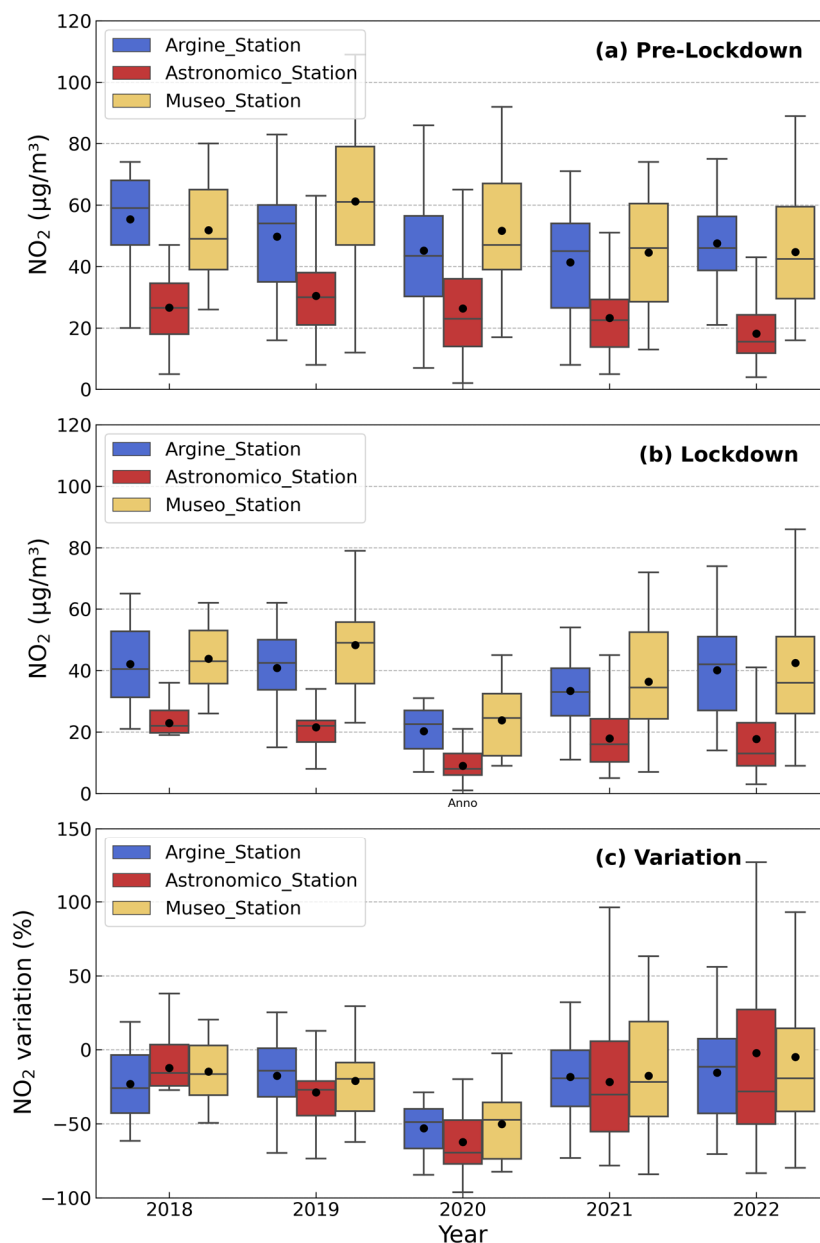


**Figure 1.** Daily averaged values of the NO<sub>2</sub> concentration as a function of the year for the pre-lockdown (panel (a)) and lockdown (panel (b)) periods and relative variation (panel (c)) as registered at the three sampling stations: Argine (blue), Astronomico (red), and Museo (yellow). The central line inside the box is the median, while the black dot is the mean. The box spans from the 1st quartile (Q1) to the 3rd quartile (Q3), showing the middle 50% of the data, while whiskers extend from the smallest to the largest values within 1.5 times the IQR, defined as the length of the box.



Figure 1c displays the relative variations for the NO<sub>2</sub> data registered by the three ARPAC stations in terms of statistical box plot, evidencing a clear negative variation in the pandemic year. The presence of this minimum suggests that the reduction in the NO<sub>2</sub> values for the year 2020 during the lockdown phase is greater than that due to any seasonal variation. Furthermore, the reduction in the pandemic year is of the same order for all three stations, thus suggesting that the observed decrease is independent of the specific features inherent to each measurement area; indeed, it highlights the peculiar conditions that occurred during the pandemic lockdown of the year 2020. Finally, Figure 1 provides a rather robust confirmation of the uniqueness of the year 2020 and displays a clear recovery trend towards a pre-pandemic situation for NO<sub>2</sub> in the following two years.

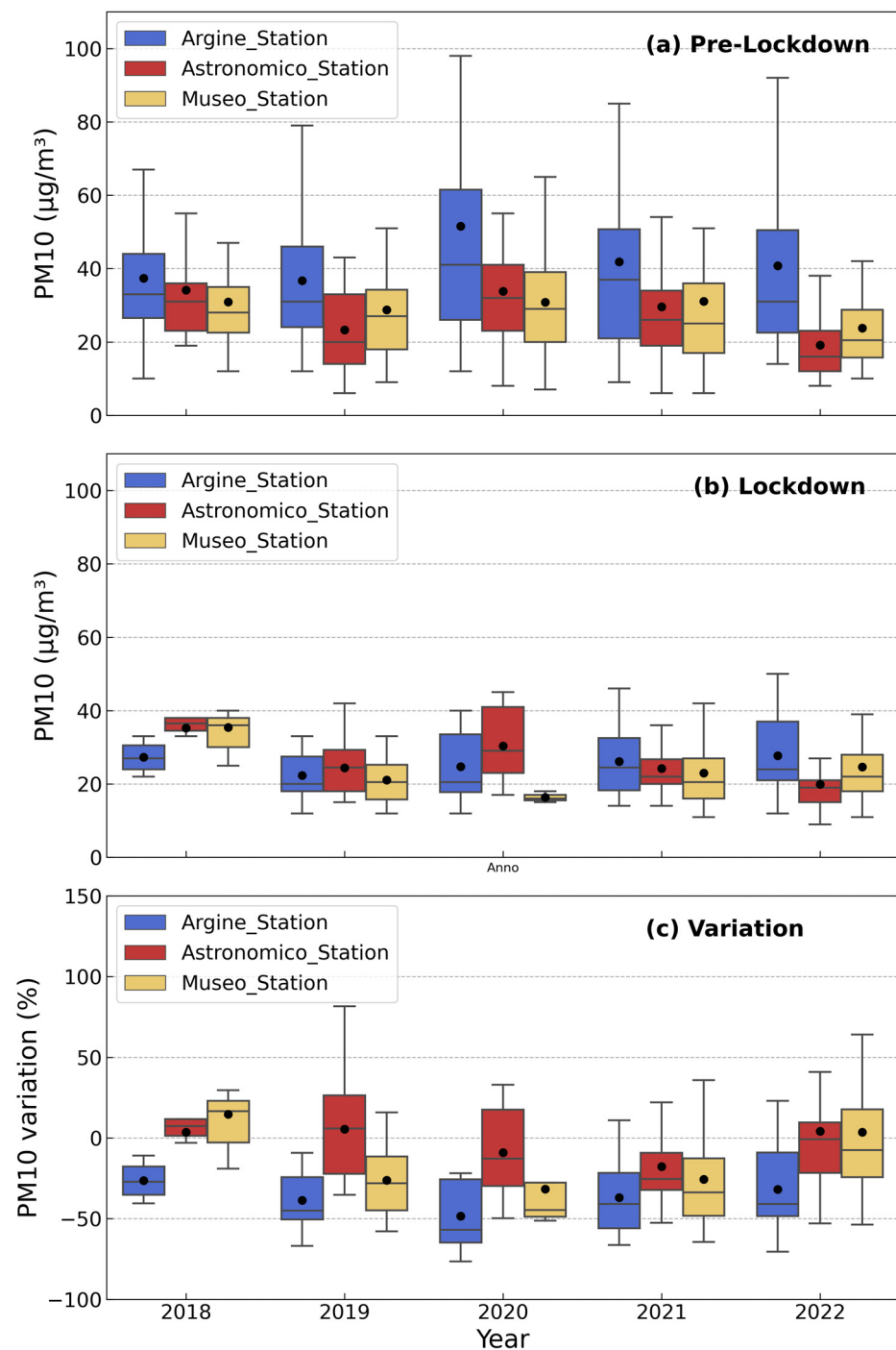
The observed variations in NO<sub>2</sub> (in percentage, reductions between 35% and 60% between 2020 and the other years during lockdown) result in good agreement with those reported in several previous studies [45,46]; for instance, satellite data revealed that the reduction in the total NO<sub>2</sub> content in the vertical atmospheric column in 2020 reached values as high as 20–40% over China, India, Malaysia, Europe, South America, and the USA [47,48]. Moreover, a 34.0% reduction in NO<sub>2</sub> concentration was estimated on the global scale by using data derived from 458 air monitoring stations on five continents [49]. Finally, the twofold decrease in NO<sub>2</sub> observed above is consistent with the reduction observed over the Campania region by sampling stations located in both urban and suburban areas or in zones affected by city traffic [27].

We turn now to the analysis of the behavior of PM<sub>10</sub>. The amount of available daily data is very similar to that for NO<sub>2</sub>. Figure 2 reports statistical box plots of the PM<sub>10</sub> concentrations registered in the pre-lockdown (Figure 2a) and lockdown (Figure 2b) periods, defined above by the three ARPAC stations, as well as their relative variations (Figure 2c). Different to NO<sub>2</sub>, the five-year comparison does not seem to show a significant difference for the pandemic year with respect to the two previous and following years. However, it is interesting to note that in the pandemic year 2020, the maximum values of the PM<sub>10</sub> concentration registered by the three stations in the lockdown period are lower than those for pre-lockdown, with the largest decrease occurring for Argine, the closest to an industrial area, followed by Museo, representative of the city center, and then by Astronomico. Moreover, the mean and median values of PM<sub>10</sub> decreased by almost two times for the Argine and Museo stations, whereas for the Astronomico sampling station, they remained at almost similar levels.

Figure 2c shows the relative variation in PM<sub>10</sub>. Even in this case, one can observe the presence of a dip in the five-year trend for the pandemic year 2020 for the Argine and Museo stations, like what was observed for NO<sub>2</sub>. For the Astronomico station, this effect is less evident; such a singular behavior might be related to the specificity of the site and agrees with what was observed in our previous work [26], where the variation in PM<sub>10</sub> was lower or even positive (increase) in the more natural areas. The variation between 2020 and other years during lockdown periods reaches values as high as 50%.

Summarizing the near-surface characterization, NO<sub>2</sub> presents a clear reduction in the pandemic year and can be assumed to be a key indicator of the changes induced by the restrictions set up during the lockdown period. In fact, anthropogenic sources of NO<sub>2</sub> are primarily emissions from transportation and fuel combustion that derive mainly from vehicle exhaust gases in urban areas [31]. The influence of the changes due to the lockdown on PM<sub>10</sub> are less evident, because it is originated by a wide range of anthropogenic and natural sources. The residential heating and the domestic consumption variation related to people forced to stay at home may have affected the PM<sub>10</sub> variation [50–52]. Moreover, the particulate matter is more affected by long-distance transport of particles of natural sources [53] and has a different residence time in the atmosphere with respect to gaseous pollutants. For this reason, it is understandable that PM<sub>10</sub> is less affected by the variation in the anthropogenic activities. Therefore, even if we have excluded days with Saharan dust events in our analysis, the contribution coming from natural sources can still play a role. However, some changes are clearly also evidenced for PM<sub>10</sub>, suggesting a variation

in its characteristics that will be further addressed in the next section, which is related to the columnar properties of the atmospheric aerosol.



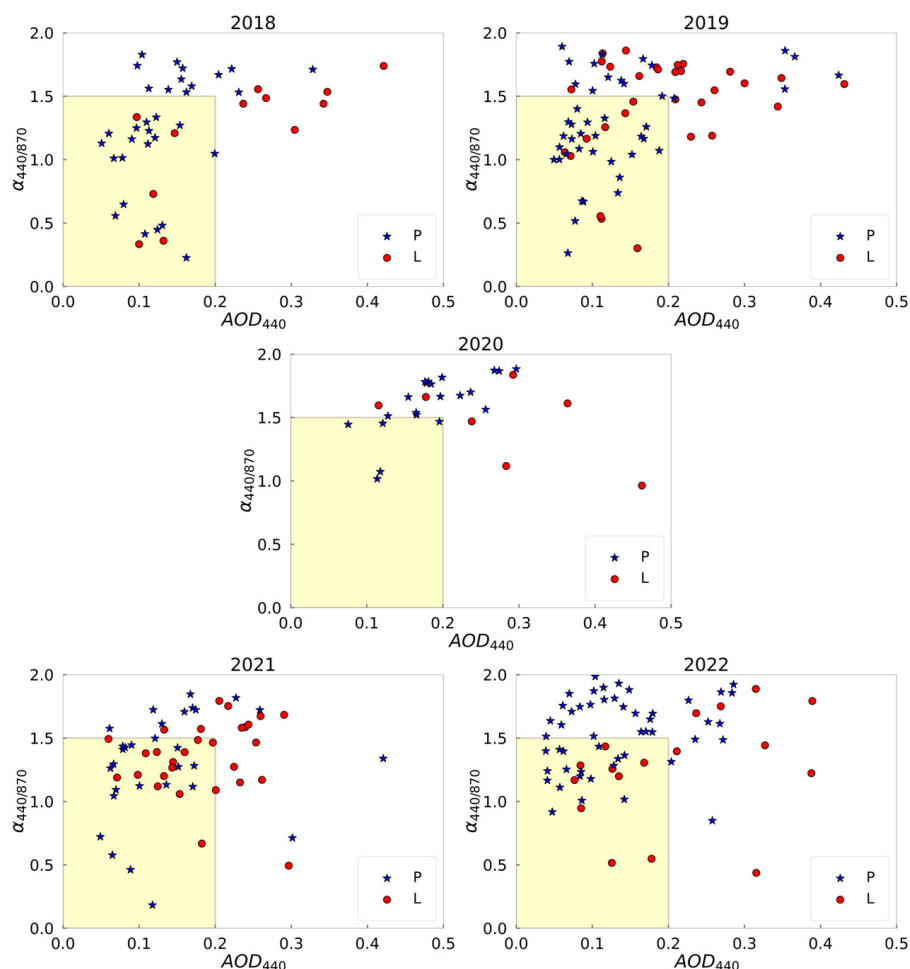
**Figure 2.** Daily averaged values of the PM10 concentration as a function of the year for the pre-lockdown (panel (a)) and lockdown (panel (b)) periods and relative variation (panel (c)) as registered at the three sampling stations: Argine (blue), Astronomico (red), and Museo (yellow). The central line inside the box is the median, while the black dot is the mean. The box spans from the 1st quartile (Q1) to the 3rd quartile (Q3), showing the middle 50% of the data, while whiskers extend from the smallest to the largest values within 1.5 times the IQR, defined as the length of the box.

Table 1 reports the mean values of AOD and  $\alpha$  registered by the sun photometer measurements. From Table 1, one can observe that the values of both AOD and  $\alpha$  are

consistent within the statistical uncertainty in each interval associated with the various years; this makes it difficult to understand a possible trend. In an attempt to gain a more reliable characterization of the type of atmospheric aerosol present in the air column, the relationship between the  $\alpha$  and AOD data can be exploited, as highlighted in [38]. Therefore, Figure 3 reports the scatter plots of the two parameters  $\alpha$  and AOD for the two periods P and L in the five-year interval, extending the comparison carried out in our previous work [26]. The panel for the pandemic year 2020 is located in the middle of Figure 3 for easiness of comparison.

**Table 1.** Mean values of AOD and  $\alpha$  registered by solar measurements in the two temporal periods P (1 January–12 March) and L (20 March–30 April) for the years 2018, 2019, 2020 (pandemic year), 2021, and 2022.

Year	AOD		$\alpha$	
	P	L	P	L
2018	$0.13 \pm 0.01$	$0.23 \pm 0.03$	$1.2 \pm 0.8$	$1.2 \pm 0.1$
2019	$0.16 \pm 0.02$	$0.19 \pm 0.02$	$1.30 \pm 0.06$	$1.43 \pm 0.07$
2020	$0.18 \pm 0.01$	$0.28 \pm 0.04$	$1.64 \pm 0.06$	$1.4 \pm 0.1$
2021	$0.15 \pm 0.02$	$0.18 \pm 0.01$	$1.28 \pm 0.07$	$1.35 \pm 0.05$
2022	$0.13 \pm 0.01$	$0.21 \pm 0.03$	$1.53 \pm 0.04$	$1.3 \pm 0.1$



**Figure 3.** Scatter plots of Angstrom coefficient ( $\alpha$ ) and aerosol optical depth (AOD) for both time intervals P (pre-lockdown) (blue dots) and L (lockdown) (red points) during the five-year period from 2018 to 2022.



Figure 3 highlights the absence of data for the period L of the lockdown year 2020 in the yellow box identified by the extremes  $0 \leq \text{AOD} \leq 0.2$  and  $0 \leq \alpha \leq 1.5$  as compared to the other four years (2018, 2019, 2021, and 2022). Differently, the yellow box is populated by 19 points for the P period and 5 points for the L one in 2018, 27 points in P-2019 and 9 in L-2019, 18 points for P-2021 and 14 for L-2021, and 17 points in P-2022 and 9 in L-2022. The highlighted range corresponds to atmospheric conditions characterized by large particles (lower  $\alpha$  values), generally associated with local soil particle uplift and polluted marine aerosol components, and large and fine anthropogenic particles, associated with vehicle emissions and anthropogenic activities [54,55]. The figure evidences an almost total reduction in a particular aerosol component whose origin can be ascribed to anthropogenic activities [26]. The recovery of such an aerosol component is also reflected in the volume size distribution, as illustrated hereafter.

Also in this case, the data referring to the days affected by dust events were removed, and the daily distributions were averaged over the observation periods. Prior to illustrating the data, we recall that in 2020, an almost threefold increase in the fine aerosol component was observed in the Naples urban area as a characteristic feature of the changes occurring in the period of the lockdown L with respect to the previous P one [26]. Interestingly, in the year 2021, the average size distributions for the two periods P and L shown in Figure 4a are indeed consistent within the experimental uncertainties. The two curves show very similar features for both fine and coarse particles, suggesting the absence of significant changes in the two observational intervals. A similar coherence of the average size distributions in the two periods was also observed for the years 2018, 2019, and 2022, thus suggesting that the peculiar behavior observed in 2020 can be reliably ascribed to the effects induced by the pandemic lockdown. The increase in the fine aerosol component in the atmospheric column during the lockdown in the year 2020 is clearly discerned in Figure 4b, which reports the size distributions observed in the five different years for the L interval. The fine component for the pandemic year 2020 appears markedly different compared to the other four years (2018, 2019, 2021, and 2022), whose features instead have very similar results. The curves clearly evidence a remarkable change in the finer fraction of the aerosol, whereas for the coarser part, the variation is lower and referable to statistical fluctuations. This observation puts into evidence an unexpected change in the atmospheric aerosol composition in the period of the lockdown, with a predominance of the finer aerosol fraction.

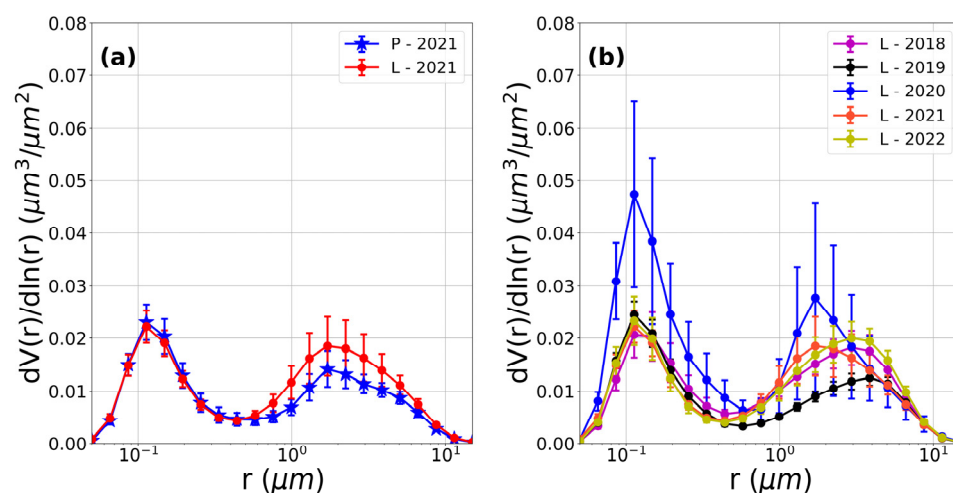


**Figure 4.** (a) Volume size distributions observed in the year 2021 for the pre-lockdown (P—2021, blue stars) and lockdown (L—2021, red dots) periods. (b) Volume size distribution for the lockdown (L) periods for the three years: 2018—magenta, 2019—black, 2020—blue, 2021—red, 2022—yellow.

Considering that fine and ultrafine fractions of PM have been associated with anthropogenic emission sources such as traffic, which suffered drastic decreases during the lockdown, the observed increase along the atmospheric column in the fine/ultrafine frac-

tion with respect to the coarse one could be associated with continental origin and more or less polluted marine components. Moreover, the closeness of the measurement area to the Solfatara natural source of SO<sub>2</sub> may also have contributed to sub-micron secondary sulphate aerosol injection in the atmosphere [26].

#### 4. Conclusions

In summary, here we extended our previous work on the air quality and aerosol compositional changes in the city of Naples due to the pandemic lockdown of the year 2020 [26]. This was addressed by following some air quality parameters over a five-year period centered on the year 2020. Our analysis allows us to further evidence the peculiar situation that occurred during the lockdown and addresses how the recovery of human social and industrial activities impacted the urban air pollution levels in the following years. Hence, it provides a unique opportunity to give clear evidence of the influence of human activities on the air quality.

The analysis was carried out by resorting to both NO<sub>2</sub> and PM<sub>10</sub> mean concentration levels measured at ground level in key points of the city and columnar data of the optical and microphysical aerosol properties provided by a sun photometer. NO<sub>2</sub> and PM<sub>10</sub> data registered at ground level in the five-year period from 2018 to 2022 were analyzed, excluding days corresponding to the Saharan dust events typically occurring in the measurement area. The experimental findings address a significant relative reduction in NO<sub>2</sub>, consistent with other reports, as well as a peculiar behavior of PM<sub>10</sub>, whose mean value at ground level seems to be less affected, but with an overall reduction in the maximum values registered in the lockdown period with respect to the same periods of the other four years. This observation suggests a change in the characteristics of the particulate matter at ground level, which is also associated with an intriguing compositional change in the atmospheric particulate that evidences a prevalence of the finer component in the lockdown period of the pandemic year 2020. These findings ascertain a clear influence of the changes in anthropogenic activities on the air quality during the lockdown period. The columnar properties of the atmospheric aerosols highlighted the absence of data corresponding to larger aerosols ( $\alpha \leq 1.5$ ) in clear atmospheric conditions ( $AOD \leq 0.2$ ) for only the 2020 lockdown period. The increase in the fine aerosol component in the atmospheric column during this period is also clearly evidenced in the aerosol size distributions. In particular, our findings highlight a predominance of finer atmospheric aerosols (mean radius of about 0.11  $\mu\text{m}$ ) during the lockdown in the year 2020 only, as a consequence of a change in the atmospheric aerosol composition.

The result obtained could be associated with local characteristics related to the presence of fumarolic aerosols due to the persistent activity of the Solfatara volcano and the consequent transformation into fine particulates of secondary aerosols produced in the atmosphere.

In conclusion, our findings highlight a significant reduction in NO<sub>2</sub> and PM<sub>10</sub> levels during the 2020 lockdown, with a gradual return to pre-pandemic levels in subsequent years. These findings underscore the impact of human activities on air quality and the potential benefits of emission reduction strategies, as they show a clear, short-term air quality improvement during the 2020 lockdown associated with a change in the mean dimension of the atmospheric aerosol; in fact, the resumption of social and industrial activities is accompanied by a recovery towards previous levels of both the pollution degree in the city and the aerosol properties in the atmospheric column. The analysis of the post-pandemic period confirms that, besides the undesired effects on human life, the lockdown represented a remarkable event, emphasizing both the direct influence of anthropic activities on the air quality and environment and the need for the development of smarter cities and policies to limit their impact.

**Author Contributions:** Conceptualization, A.S. and R.D.; methodology, A.S. and R.D.; software, P.C.; validation, A.S. and R.D.; formal analysis, A.S. and R.D.; investigation, A.S. and R.D.; resources, M.D.; data curation, A.S. and R.D.; writing—original draft preparation, A.S. and R.D.; writing—review and editing, A.B. and S.A.; visualization, A.S. and R.D.; supervision, A.B. and S.A.; project administration, A.B. and S.A.; funding acquisition, A.B. and S.A. A.S. and R.D. contributed equally to this work. All authors have read and agreed to the published version of the manuscript.

**Funding:** This research was funded by the European Union’s Horizon 2020 research and innovation program under grant agreement No. 654109, ACTRIS2 project.

**Data Availability Statement:** The data presented in this study are available on request from the corresponding author.

**Acknowledgments:** The authors gratefully acknowledge the NOAA Air Resource Laboratory (ARL) for providing the HYSPLIT transport and dispersion model and/or READY website used in this publication. Data from the BSC-DREAM8b (Dust Regional Atmospheric Model) model were operated by the Barcelona Supercomputing Center (<http://www.bsc.es/ess/bsc-dust-daily-forecast/>), accessed on 14 June 2024). The authors also acknowledge ARPAC for providing atmospheric air pollution data.

**Conflicts of Interest:** Pasquale Castellano was employed by the company ALA Advanced Lidar Applications s.r.l. The remaining authors declare that the research was conducted in the absence of any commercial or financial relationships that could be construed as a potential conflict of interest.

## References

1. Gu, X.; Lin, C.; Wang, B.; Wang, J.; Ouyang, W. A comprehensive assessment of anthropogenic impacts, contamination, and ecological risks of toxic elements in sediments of urban rivers: A case study in Qingdao, East China. *Environ. Adv.* **2022**, *7*, 100143. [[CrossRef](#)]
2. Ellis Erle, C. Anthropogenic transformation of the terrestrial biosphere. *Philos. Trans. R. Soc. A* **2011**, *369*, 1010–1035. [[CrossRef](#)]
3. Halpern, B.S.; Walbridge, S.; Selkoe, K.A.; Kappel, C.V.; Micheli, F.; D’Agrosa, C.; Bruno, J.F.; Casey, K.S.; Ebert, C.; Fox, H.E.; et al. A Global Map of Human Impact on Marine Ecosystems. *Science* **2008**, *319*, 948–952. [[CrossRef](#)]
4. McMichael, A.J.; Woodruff, R.E.; Hales, S. Climate change and human health: Present and future risks. *Lancet* **2006**, *367*, 859–869. [[CrossRef](#)]
5. Keesing, F.; Belden, L.K.; Daszak, P.; Dobson, A.; Harvell, C.D.; Holt, R.D.; Hudson, P.; Jolles, A.E.; Jones, K.E.; Mitchell, C.E.; et al. Impacts of biodiversity on the emergence and transmission of infectious diseases. *Nature* **2010**, *468*, 647–652. [[CrossRef](#)]
6. Tovar, A.; Moreno, C.; Manuel-Vez, M.P.; García-Vargas, M. Environmental impacts of intensive aquaculture in marine waters. *Water Res.* **2000**, *34*, 334–342. [[CrossRef](#)]
7. Gorte, R.W.; Sheikh, P.A. *Deforestation and Climate Change*; Congressional Research Service: Washington, DC, USA, 2010; Volume 11, pp. 21–23, 9p.
8. Solomon, S.; Daniel, J.S.; Sanford, T.J.; Murphy, D.M.; Plattner, G.K.; Knutti, R.; Friedlingstein, P. Persistence of climate changes due to a range of greenhouse gases. *Proc. Natl. Acad. Sci. USA* **2010**, *107*, 18354–18359. [[CrossRef](#)]
9. Douglas, P.; Robertson, S.; Gay, R.; Hansell, A.L.; Gant, T.W. A systematic review of the public health risks of bioaerosols from intensive farming. *Int. J. Hyg. Environ. Health* **2018**, *221*, 134–173. [[CrossRef](#)]
10. Foti, G.; Barbaro, G.; Barilla, G.C.; Frega, F. Effects of Anthropogenic Pressures on Dune Systems—Case Study: Calabria (Italy). *J. Mar. Sci. Eng.* **2022**, *10*, 10. [[CrossRef](#)]
11. Defrance, D.; Ramstein, G.; Charbit, S.; Vrac, M.; Famien, A.M.; Sultan, B.; Swingedouw, D.; Dumas, C.; Gemenne, F.; Alvarez-Solas, J.; et al. Consequences of rapid ice sheet melting on the Sahelian population vulnerability. *Proc. Natl. Acad. Sci. USA* **2017**, *114*, 6533–6538. [[CrossRef](#)]
12. Moreno-Mateos, D.; Barbier, E.B.; Jones, P.C.; Jones, H.P.; Aronson, J.; López-López, J.A.; McCrackin, M.L.; Meli, P.; Montoya, D.; Rey Benayas, J.M. Anthropogenic ecosystem disturbance and the recovery debt. *Nat. Commun.* **2017**, *8*, 14163. [[CrossRef](#)]
13. Arif, M.; Kumar, R.; Parveen, S.; Singh, K.K.; Singh, J. Reduction in Environmental Pollution Due to Lockdown in the COVID-19 Pandemic: A Case Study of Delhi-NCR. In *Stakeholder Strategies for Reducing the Impact of Global Health Crises*; IGI Global: Hershey, PA, USA, 2021; pp. 239–255. [[CrossRef](#)]
14. Rume, T.; Islam, S.D.U. Environmental effects of COVID-19 pandemic and potential strategies of sustainability. *Heliyon* **2020**, *6*, e04965. [[CrossRef](#)]
15. Yunus, A.P.; Masago, Y.; Hijioka, Y. COVID-19 and surface water quality: Improved lake water quality during the lockdown. *Sci. Total Environ.* **2020**, *731*, 139012. [[CrossRef](#)]
16. Obregón, M.Á.; Martín, B.; Serrano, A. Footprint of the 2020 COVID-19 Lockdown on Column-Integrated Aerosol Parameters in Spain. *Remote Sens.* **2023**, *15*, 3167. [[CrossRef](#)]
17. Romano, S.; Catanzaro, V.; Paladini, F. Impacts of the COVID-19 Lockdown Measures on the 2020 Columnar and Surface Air Pollution Parameters over South-Eastern Italy. *Atmosphere* **2021**, *12*, 1366. [[CrossRef](#)]

18. Tokatlı, C.; Varol, M. Impact of the COVID-19 lockdown period on surface water quality in the Meriç-Ergene River Basin, Northwest Turkey. *Environ. Res.* **2021**, *197*, 111051. [[CrossRef](#)]
19. Ethan, C.J.; Mokoena, K.K.; Yu, Y. Air Quality Status in Wuhan City during and One Year after the COVID-19 Lockdown. *Aerosol Air Qual. Res.* **2022**, *22*, 210282. [[CrossRef](#)]
20. Menut, L.; Bessagnet, B.; Siour, G.; Mailler, S.; Pennel, R.; Cholakian, A. Impact of lockdown measures to combat COVID-19 on air quality over western Europe. *Sci. Total Environ.* **2020**, *741*, 140426. [[CrossRef](#)]
21. Begou, P.; Evagelopoulos, V.; Charisiou, N.D. Variability of air pollutant concentrations and their relationships with meteorological parameters during COVID-19 lockdown in western macedonia. *Atmosphere* **2023**, *14*, 1398. [[CrossRef](#)]
22. Kerimray, A.; Baimatova, N.; Ibragimova, O.P.; Bukenov, B.; Kenessov, B.; Plotitsyn, P.; Karaca, F. Assessing air quality changes in large cities during COVID-19 lockdowns: The impacts of traffic-free and reduced anthropogenic activities. *Environ. Pollut.* **2020**, *266*, 115017. [[CrossRef](#)]
23. He, G.; Pan, Y.; Tanaka, T. The short-term impacts of COVID-19 lockdown on urban air pollution in China. *Nat. Sustain.* **2020**, *3*, 1005–1011. [[CrossRef](#)]
24. Wang, K.; Zhao, X. The Impact of COVID-19 Lockdowns on Satellite-Observed Aerosol Optical Thickness over the Surrounding Coastal Oceanic Areas of Megacities in the Coastal Zone. *Geographies* **2021**, *1*, 381–397. [[CrossRef](#)]
25. Bahukhandi, K.; Agarwal, S.; Singhal, S. Impact of lockdown COVID-19 pandemic on himalayan environment. *Int. J. Environ. Anal. Chem.* **2023**, *103*, 326–340. [[CrossRef](#)]
26. Sannino, A.; D’Emilio, M.; Castellano, P.; Amoruso, S.; Boselli, A. Analysis of Air Quality during the COVID-19 Pandemic Lockdown in Naples (Italy). *Aerosol Air Qual. Res.* **2021**, *21*, 200381. [[CrossRef](#)]
27. Cardito, A.; Carotenuto, M.; Amoruso, A.; Libralato, G.; Lofrano, G. Air quality trends and implications pre and post COVID-19 restrictions. *Sci. Total Environ.* **2023**, *879*, 162833. [[CrossRef](#)] [[PubMed](#)]
28. Gamal, G.; Abdeldayem, O.M.; Elattar, H.; Hendy, S.; Gabr, M.E.; Mostafa, M.K. Remote Sensing Surveillance of NO<sub>2</sub>, SO<sub>2</sub>, CO, and AOD along the Suez Canal Pre- and Post-COVID-19 Lockdown Periods and during the Blockage. *Sustainability* **2023**, *15*, 9362. [[CrossRef](#)]
29. ARPAC. 2021. Available online: [www.arpacampania.it](http://www.arpacampania.it) (accessed on 13 February 2024).
30. Shi, Z.B.; Song, C.B.; Liu, B.W.; Lu, G.D.; Xu, J.S.; Vu, T.V.; Elliott, R.J.R.; Li, W.J.; Bloss, W.J.; Harrison, R.M. Abrupt but smaller than expected changes in surface air quality attributable to COVID-19 lockdowns. *Sci. Adv.* **2021**, *7*, eabd6696. [[CrossRef](#)]
31. Copat, C.; Cristaldi, A.; Fiore, M.; Grasso, A.; Zuccarello, P.; Signorelli, S.S.; Conti, G.O.; Ferrante, M. The role of air pollution (PM and NO<sub>2</sub>) in COVID-19 spread and lethality: A systematic review. *Environ. Res.* **2020**, *191*, 110129. [[CrossRef](#)] [[PubMed](#)]
32. Meng, X.; Liu, C.; Chen, R.; Sera, F.; Vicedo-Cabrera, A.M.; Milojevic, A.; Guo, Y.; Tong, S.; Coelho, M.d.S.Z.S.; Saldiva, P.H.N.; et al. Short term associations of ambient nitrogen dioxide with daily total, cardiovascular, and respiratory mortality: Multilocation analysis in 398 cities. *BMJ* **2021**, *372*, n534. [[CrossRef](#)]
33. Speranza, A.; Caggiano, R. Impacts of the COVID-19 lockdown measures on coarse and fine atmospheric aerosol particles (PM) in the city of Rome (Italy): Compositional data analysis approach. *Air Qual. Atmos. Health* **2022**, *15*, 2035–2050. [[CrossRef](#)]
34. Holben, B.N.; Eck, T.F.; Slutsker, I.; Tanré, D.; Buis, J.P.; Setzer, A.; Vermote, E.; Reagan, J.A.; Kaufman, Y.J.; Nakajima, T.; et al. AERONET—A Federated Instrument Network and Data Archive for Aerosol Characterization. *Remote Sens. Environ.* **1998**, *66*, 1–16. [[CrossRef](#)]
35. Brogniez, C.; Lenoble, J.; Shaw, G. Direct observation of the sun for aerosol retrieval. In *Aerosol Remote Sensing*; Lenoble, J., Remer, L., Tanre, D., Eds.; Springer: Berlin/Heidelberg, Germany, 2013; pp. 87–99. [[CrossRef](#)]
36. Dubovik, O.; King, M.D. A flexible inversion algorithm for the retrieval of aerosol optical properties from sun and sky radiance measurements. *J. Geophys. Res.* **2000**, *105*, 20673–20696. [[CrossRef](#)]
37. Di Antonio, L.; Di Biagio, C.; Foret, G.; Formenti, P.; Siour, G.; Doussin, J.-F.; Beekmann, M. Aerosol optical depth climatology from the high-resolution MAIAC product over Europe. *Atmos. Chem. Phys.* **2023**, *23*, 12455–12475. [[CrossRef](#)]
38. Kaskaoutis, D.G.; Kambezidis, H.D.; Adamopoulos, A.D.; Kassomenos, P.A. On the characterization of aerosols using the Ångström exponent in the Athens area. *J. Atmos. Sol.-Terr. Phys.* **2006**, *68*, 2147–2163. [[CrossRef](#)]
39. Eck, T.; Holben, B.N.; Reid, J.; Dubovik, O.; Smirnov, A.; Neill Slutsker, I.; Kinne, S. Wavelength dependence of the optical depth of biomass burning, urban, and desert dust aerosols. *J. Geophys. Res. Atmos.* **1999**, *104*, 31333–31349. [[CrossRef](#)]
40. Russell, P.B.; Bergstrom, R.W.; Shinzuka, Y.; Clarke, A.D.; DeCarlo, P.F.; Jimenez, J.L.; Livingston, J.M.; Redemann, J.; Dubovik, O.; Strawa, A. Absorption Angstrom Exponent in AERONET and related data as an indicator of aerosol composition. *Atmos. Chem. Phys.* **2010**, *10*, 1155–1169. [[CrossRef](#)]
41. Boselli, A.; Caggiano, R.; Cornacchia, C.; Madonna, F.; Mona, L.; Macchiato, M.; Pappalardo, G.; Trippetta, S. Multi year sun-photometer measurements for aerosol characterization in a Central Mediterranean site. *Atmos. Res.* **2012**, *104–105*, 98–110. [[CrossRef](#)]
42. Sorrentino, A.; Sannino, A.; Spinelli, N.; Piana, M.; Boselli, A.; Tontodonato, V.; Castellano, P.; Wang, X. A Bayesian parametric approach to the retrieval of the atmospheric number size distribution from lidar data. *Atmos. Meas. Tech.* **2022**, *15*, 149–164. [[CrossRef](#)]
43. Dubovik, O.; Holben, B.N.; Lapyonok, T.; Sinyuk, A.; Mishchenko, M.I.; Yang, P.; Slutsker, I. Non-spherical aerosol retrieval method employing light scattering by spheroids. *Geophys. Res. Lett.* **2002**, *29*, 54-1–54-4. [[CrossRef](#)]

44. Giles, D.M.; Sinyuk, A.; Sorokin, M.G.; Schafer, J.S.; Smirnov, A.; Slutsker, I.; Eck, T.F.; Holben, B.N.; Lewis, J.R.; Campbell, J.R.; et al. Advancements in the Aerosol Robotic Network (AERONET) Version 3 database—Automated near-real-time quality control algorithm with improved cloud screening for Sun photometer aerosol optical depth (AOD) measurements. *Atmos. Meas. Tech.* **2019**, *12*, 169–209. [[CrossRef](#)]
45. Silva, A.C.T.; Branco, P.T.B.S.; Sousa, S.I.V. Impact of COVID-19 Pandemic on Air Quality: A Systematic Review. *Int. J. Environ. Res. Public Health* **2022**, *19*, 1950. [[CrossRef](#)] [[PubMed](#)]
46. Pushpawela, B.; Shelton, S.; Liyanage, G.; Jayasekara, S.; Rajapaksha, D.; Jayasundara, A.; Jayasuriya, L.D. Changes of Air Pollutants in Urban Cities during the COVID-19 Lockdown-Sri Lanka. *Aerosol Air Qual. Res.* **2023**, *23*, 220223. [[CrossRef](#)]
47. Filonchik, M.; Hurynovich, V.; Yan, H.; Gusev, A.; Shpilevskaya, N. Impact Assessment of COVID-19 on Variations of SO<sub>2</sub>, NO<sub>2</sub>, CO and AOD over East China. *Aerosol Air Qual. Res.* **2020**, *20*, 1530–1540. [[CrossRef](#)]
48. Oo, T.K.; Arunrat, N.; Kongsurakan, P.; Sereenonchai, S.; Wang, C. Nitrogen Dioxide (NO<sub>2</sub>) Level Changes during the Control of COVID-19 Pandemic in Thailand. *Aerosol Air Qual. Res.* **2021**, *21*, 200440. [[CrossRef](#)]
49. Torkmahalleh, M.A.; Akhmetvaliyeva, Z.; Omran, A.D.; Omran, F.F.D.; Kazemitabar, M.; Naseri, M.; Naseri, M.; Sharifi, H.; Malekipirbazari, M.; Adotey, E.K.; et al. Global air quality and COVID-19 pandemic: Do we breathe cleaner air? *Aerosol Air Qual. Res.* **2021**, *21*, 200567. [[CrossRef](#)]
50. Querol, X.; Alastuey, A.; Ruiz, C.R.; Artiñano, B.; Hansson, H.C.; Harrison, R.M.; Buringh, E.; ten Brink, H.M.; Lutz, M.; Bruckmann, P.; et al. Speciation and origin of PM<sub>10</sub> and PM<sub>2.5</sub> in selected European cities. *Atmos. Environ.* **2004**, *38*, 6547–6555. [[CrossRef](#)]
51. Pültz, J.; Banzhaf, S.; Thürkow, M.; Kranenburg, R.; Schaap, M. Source attribution of particulate matter in Berlin. *Atmos. Environ.* **2022**, *292*, 119416. [[CrossRef](#)]
52. Chan, E.C.; Jäkel, I.J.; Khan, B.; Schaap, M.; Butler, T.M.; Forkel, R.; Banzhaf, S. An enhanced emissions module for the PALM model system 23.10 with application on PM<sub>10</sub> emissions from urban domestic heating. *Geosci. Model Dev. Discuss.* **2024**, preprint. [[CrossRef](#)]
53. Millán-Martínez, M.; Sánchez-Rodas, D.; Sánchez de la Campa, A.M.; de la Rosa, J. Contribution of anthropogenic and natural sources in PM<sub>10</sub> during North African dust events in Southern Europe. *Environ. Pollut.* **2021**, *290*, 118065. [[CrossRef](#)]
54. Toledano, C.; Cachorro, V.E.; Berjon, A.; de Frutos, A.M.; Sorribas, M.; de la Morena, B.A.; Goloub, P. Aerosol optical depth and Angstrom exponent climatology at El Arenosillo AERONET site (Huelva, Spain). *Q. J. R. Meteorol. Soc.* **2007**, *133*, 795–807. [[CrossRef](#)]
55. Pavese, G.; Lettino, A.; Calvello, M.; Esposito, F.; Fiore, S. Aerosol composition and properties variation at the ground and over the column under different air masses advection in South Italy. *Environ. Sci. Pollut. Res. Int.* **2016**, *23*, 6546–6562. [[CrossRef](#)] [[PubMed](#)]

**Disclaimer/Publisher’s Note:** The statements, opinions and data contained in all publications are solely those of the individual author(s) and contributor(s) and not of MDPI and/or the editor(s). MDPI and/or the editor(s) disclaim responsibility for any injury to people or property resulting from any ideas, methods, instructions or products referred to in the content.